Periportal and pericentral pyridine nucleotide fluorescence from the surface of the perfused liver: Evaluation of the hypothesis that chronic treatment with ethanol produces pericentral hypoxia

(lobular oxygen gradient/ethanol toxicity/liver injury/tissue oxygen tension/tissue NADH fluorescence)

SUNGCHUL JI*†, JOHN J. LEMASTERS‡, VICKIE CHRISTENSON*, AND RONALD G. THURMAN*

Departments of *Pharmacology and ‡Anatomy, School of Medicine, University of North Carolina at Chapel Hill, Chapel Hill, North Carolina 27514

ABSTRACT   Pyridine nucleotide fluorescence made from the surface of the hemoglobin-free perfused rat liver was measured continuously by using a "micro-light guide" placed on selected periportal and pericentral regions of the liver lobule. From the portal oxygen tension at which pyridine nucleotide reduction first occurred in pericentral regions, the oxygen gradient across the liver lobule was estimated in livers from rats treated chronically with ethanol or sucrose. Chronic treatment with ethanol increased the average lobular oxygen gradient from 275 to 400 torr (1 torr = 133 Pa), primarily due to the increase in the oxygen gradient in pericentral regions. Ethanol treatment also increased hepatic oxygen uptake significantly, from 110 to 144 (μmol/g)/hr. Treatment with the antithyroid drug 6-propyl-2-thiouracil reversed the effect of ethanol on O_2 uptake and on the lobular oxygen gradient. The oxygen gradients measured with the micro-light guide were confirmed by direct measurement of tissue oxygen tensions in periportal and pericentral areas by using an oxygen electrode. These data are consistent with the hypothesis that chronic treatment with ethanol causes the pericentral region of the liver lobule to become susceptible to hypoxic cellular injury. This may be responsible, at least in part, for the localized hepatotoxic effects of ethanol.

Ethanol-induced liver damage is often confined to the pericentral region of the liver lobule (1–3). Israel et al. (3) have postulated that ethanol-induced pericentral necrosis results from an accentuated gradient of decreasing oxygen tension from the portal to the central venous end of the sinusoid leading to pericentral hypoxia. This hypothesis is based on the observations that ethanol treatment increased the rate of oxygen uptake in liver slices (4–6) and perfused liver (7, 8). In support of this postulate, Israel et al. (3) demonstrated that, after brief exposure to hypoxia, pericentral necrosis was greater in ethanol-treated rats than in controls. Treatment of rats with the antithyroid drug 6-propyl-2-thiouracil abolished the ethanol-induced increase in liver respiration and diminished the tissue damage produced by hypoxia (3).

We have used a "micro-light guide" fluorometric technique (9–12) to test this hypothesis directly. This technique allows continuous measurement of pyridine nucleotide fluorescence from the periportal or pericentral regions of the perfused liver. Chance and co-workers (13, 14) have shown that tissue pyridine nucleotide fluorescence can be used to monitor intracellular oxygen tension indirectly because pyridine nucleotide fluorescence increases when tissue oxygen tension falls below the level (<1 torr; 1 torr = 133 Pa) necessary to satisfy the oxygen requirement of mitochondrial cytochrome oxidase. By measuring

the oxygen tension in the influent perfusate at which pyridine nucleotide fluorescence begins to increase in pericentral regions, it is possible to estimate the oxygen gradient across the liver lobule. The results of the present study indicate that the lobular oxygen gradient increases by about 30% in livers from rats treated chronically with ethanol. This effect of chronic ethanol treatment on the lobular oxygen gradient was confirmed by direct measurement of sublobular oxygen tension by using an oxygen electrode. Treatment with 6-propyl-2-thiouracil reversed the effect of ethanol. Preliminary accounts of this work have appeared elsewhere (15).

MATERIALS AND METHODS

Female Sprague–Dawley rats (200–250 g) received 25% (vol/vol) ethanol in 25% (wt/vol) sucrose/H_2O for 4–6 wk prior to experiments, as described by Porta et al. (16). Control rats received 25% (wt/vol) sucrose/tap water; both groups of rats had free access to laboratory chow. Livers were perfused with Krebs–Henseleit bicarbonate buffer (pH 7.6) at 37°C as described by Scholz et al. (17). Oxygen tension in the influent and effluent perfusate was measured continuously with Clark type oxygen electrodes. Rates of oxygen uptake were calculated from the difference between the influent and the effluent oxygen concentrations, the flow rate, and the liver wet weight.

Tissue pyridine nucleotide fluorescence (366 → 450 nm) was monitored from the surface of the perfused rat liver by using a micro-light guide as described (9–12). Fluorescence was observed from a disk of tissue with approximate dimensions of 240 × 90 × 130 μm and a total volume of 3 × 10^6 μm³ (11, 12).

An oxygen electrode with a tip diameter of 60–80 μm was prepared by inserting a 50-μm-diameter platinum wire into a glass capillary that was pulled under heat. The tip was coated with Rhoplex (Rhom and Haase, Philadelphia). A Ag/AgCl electrode served as the reference electrode. The electrode was calibrated with 0%, 21%, and 95% O_2 at the liver surface after perfusion fixation with 1% formaldehyde. The oxygen sensitivity of the electrode at the surface of the fixed liver was about 0.05 nA/torr, and the 90% response time was 5–10 sec.

Periportal and pericentral regions of the liver lobule were identified from the pattern of surface pigmentation of the perfused liver as described for livers from phenobarbital-treated rats (11, 12). We identified lightly pigmented areas as periportal regions and darkly pigmented spots as pericentral regions. Infusion of india ink confirmed these identifications in both sucrose- and ethanol-treated rats (Fig. 1).

† Present address: Dept. of Pharmacology, School of Pharmacy, Rutgers, The State University of New Jersey, Piscataway, NJ 08854
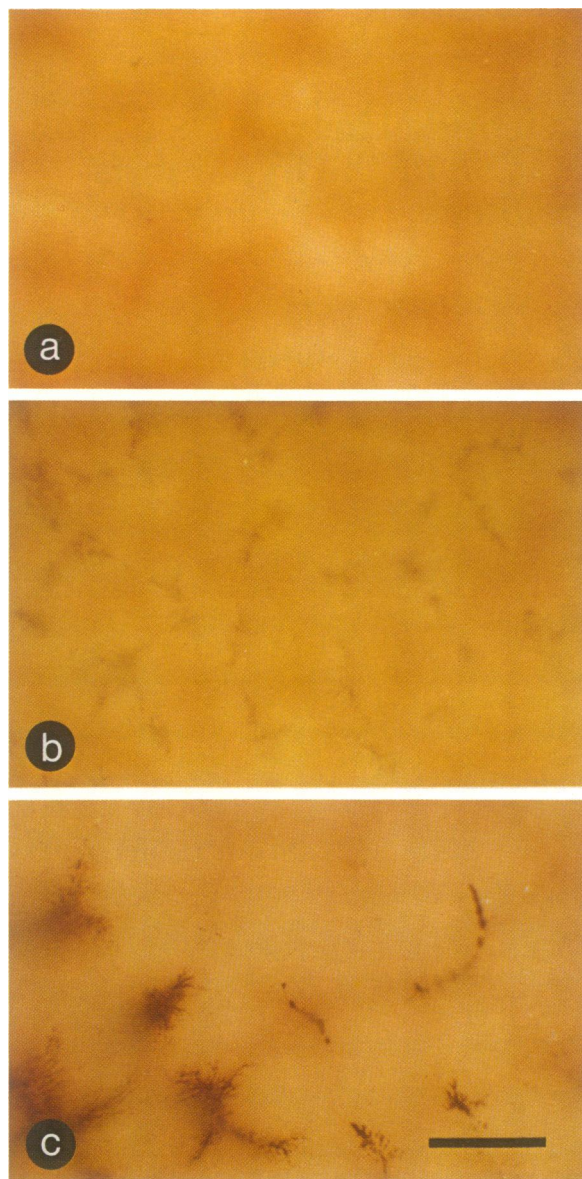
FIG. 1. Photomicrographs of perfused liver surface of a sucrose-treated rat before and after perfusion with india ink. (a) Note pigmented dark spots and light areas present before india ink infusion. (b) India ink was infused via the portal vein and flow was stopped as soon as ink appeared at the liver surface. Note that the ink has entered the light areas surrounding the pigmented dark spots. (c) India ink was infused via the vena cava. India ink staining appeared first within the dark pigmented spots. Similar results (not shown) were obtained with livers from ethanol-treated rats. Bar = 200 μm.

RESULTS

Typical responses of the pericentral and periportal regions of the liver lobule to a cycle of anoxia are shown in Fig. 2. The basal fluorescence of tissue pyridine nucleotides was considerably higher in the periportal than in the pericentral regions of the liver lobule (Fig. 2a; Table 1). Under normal perfusion conditions, influent pO_2 values were about 600 torr and effluent pO_2 values were about 200 torr (Figs. 2 and 3 b and c).

When nitrogen instead of oxygen was bubbled through the perfusion fluid reservoir, a rapid decrease in influent pO_2 occurred, followed by a decrease in effluent pO_2 after a short lag time (Fig. 2). Pyridine nucleotide fluorescence of the liver tissue began to increase when the oxygen tension in the influent perfusate decreased to less than 200–400 torr. The rate of in-
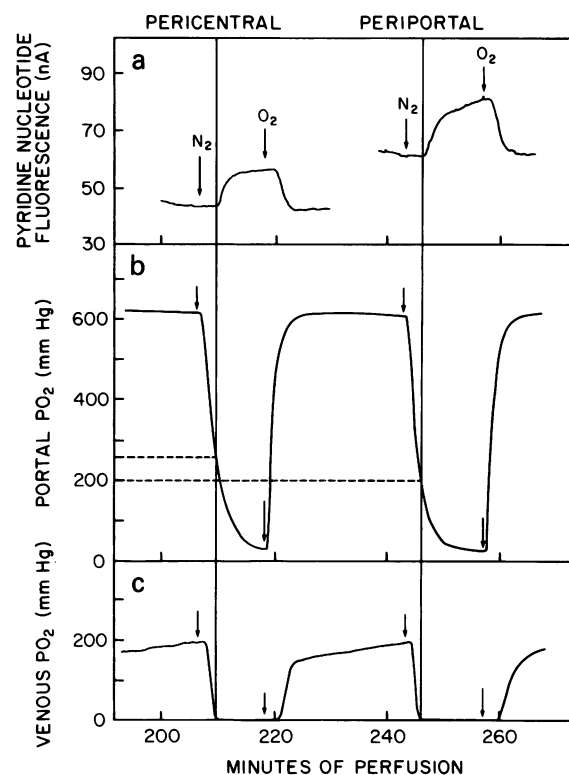

FIG. 2. Dynamic fluorescence responses (a) of periportal and pericentral areas to anoxic perfusion in livers from sucrose-treated rats. The 170-μm-tip micro-light guide was placed on a dark spot (pericentral) or a light area (periportal) on the surface of the perfused liver with a flexible mechanical arm. ↓, Times at which the equilibrating gas was changed to 95% N_2/5% CO_2 (N_2) or 95% O_2/5% CO_2 (O_2). Influent (b) and effluent (c) oxygen tensions were monitored continuously with Clark type oxygen electrodes. Pyridine nucleotide fluorescence was measured as described (9–12). Vertical lines allow estimation of input pO_2 values (see dotted lines) at which pyridine nucleotide reduction began in periportal and pericentral regions. Typical representative experiment.

crease in pyridine nucleotide fluorescence was nearly twice as fast in the pericentral region as in the periportal region (Figs. 2 and 3; Table 1). When oxygen was restored to the perfusate, all parameters returned to their respective baselines. Reoxidation of pyridine nucleotides proceeded about twice as fast in the periportal region of the liver as in the pericentral region (Table 1).

The influent pO_2 at which the fluorescence of the pericentral region began to increase approximates the oxygen gradient across the liver lobule (lobular oxygen gradient), while the pO_2 at which the fluorescence of periportal region began to increase reflects the oxygen gradient mostly confined within the periportal portion of the liver lobule (periportal oxygen gradient). The difference between the lobular gradient and the periportal gradient represents the pericentral oxygen gradient (see *Discussion*). In livers from sucrose-treated rats, the lobular oxygen gradient averaged 275 torr with an intralobular distribution of 208 torr in the periportal region and 67 torr in the pericentral area (Table 2). After ethanol treatment, the lobular oxygen gradient increased to 400 torr, primarily due to an increase in the pericentral region. This 45% increase in the oxygen gradient was accompanied by a similar increase in hepatic oxygen uptake. Treatment with 6-propyl-2-thiouracil prevented both the increase in the lobular oxygen gradient and the increase in hepatic oxygen uptake (Table 2).

Tissue oxygen tensions in periportal and pericentral regions

Table 1. Kinetic parameters of pyridine nucleotide fluorescence changes induced by anoxic cycle

	Control		Ethanol-treated	
Parameter	Periportal	Pericentral	Periportal	Pericentral
Basal fluorescence, nA	53 ± 1	40 ± 2	51 ± 2	47 ± 1*
Fluorescence increase due to N_2, %				
basal fluorescence	22 ± 3	23 ± 4	23 ± 2	27 ± 2
Initial rate of fluorescence increase				
after N_2, % basal fluorescence/min	20 ± 4	42 ± 8	16 ± 3	34 ± 4
Half-time of fluorescence increase, sec	112 ± 9	82 ± 6	117 ± 7	82 ± 4
Half-time of fluorescence decrease				
after reoxygenation, sec	60 ± 5	108 ± 8	67 ± 6	104 ± 5

Results are mean ± SEM for groups of five livers. Experimental details were similar to those in Fig. 2.
* Significantly different from control; $P < 0.01$ (Student's t test).

were measured directly by using an oxygen electrode. At a constant inflow pO_2 of about 630 torr, tissue pO_2 values measured on periportal regions from sucrose- and ethanol-treated rats were both approximately 350 torr (Table 3). When the oxygen electrode was placed on pericentral tissue, oxygen tensions of 271 and 204 torr were obtained from sucrose- and ethanol-treated rats, respectively. Periportal, pericentral, and total lobular oxygen gradients calculated from the oxygen electrode data agreed closely with the oxygen gradients calculated from NADH fluorescence measurements made with the micro-light guide (Tables 2 and 3).

DISCUSSION

Estimation of Lobular Oxygen Gradient from Pyridine Nucleotide Fluorescence. Oxygen-carrying blood enters the liver via the hepatic artery and portal vein, passes through the periportal (zone 1 of Rappaport; ref. 18) and pericentral (zone 3)

FIG. 3. Measurement of input pO_2 values corresponding to initial pyridine nucleotide reduction in periportal or pericentral regions of the liver from a chronically ethanol-treated rat. Experimental procedures were similar to those in Fig. 2. Typical representative experiment.

regions of the liver lobule, and exits the organ by the hepatic vein. Krogh (19) and others (20–22) have established that the oxygen gradient in tissue is dependent on the rate of tissue oxygen uptake, the diffusion coefficient and solubility of oxygen in tissue, and the rate of convective transport processes (microcirculation) in the vascular bed. By using a multi-wire surface oxygen electrode, Kessler and co-workers (23, 24) demonstrated that the distribution of oxygen tension on the liver surface is heterogeneous; oxygen tension values ranged from 0 to 60 torr in the liver *in situ* (23) and from 100 to 500 torr in the hemoglobin-free perfused liver (24). Although these observations indicated that oxygen gradients exist in liver tissue, no attempt was made to correlate oxygen tension with the anatomical structure of the liver lobule.

Chance and co-workers (13, 25) demonstrated that pyridine nucleotide fluorescence can be used to monitor tissue oxygenation. This technique is based on the fact that intracellular reduced pyridine nucleotides (NADH and NADPH), but not their oxidized counterparts, are fluorescent at 450 nm on excitation with light at 366 nm. This fluorescence is indirectly dependent on the intracellular oxygen tension since NADH is oxidized predominantly via the mitochondrial electron transport chain. The mitochondrial electron transport chain has an extremely high affinity for oxygen. In isolated mitochondria, the concentration of oxygen required for half-maximal electron transport is much less than 1 μM (or less than 0.75 torr) (14, 26). Thus, if mitochondria in the perfused liver tissue behave similarly to isolated mitochondria, an increase in pyridine nucleotide fluorescence can be equated with a virtual absence of oxygen at the site of fluorescence increase.

Chance *et al.* (27) measured the distribution of pyridine nucleotide fluorescence intensities in small cubes of tissue isolated from freeze-trapped liver. They observed an inhomogeneous distribution of fluorescence intensities but did not correlate the optical data with the anatomical structure of the liver. In contrast, NAD^+ and NADH contents determined by quantitative histochemistry were distributed uniformly over the liver lobule (28). The reason for this discrepancy is not known.

To understand the relationship between tissue oxygen tension and the structure of the liver, we recently modified the micro-light guide originally developed by Ji *et al.* (11, 12) so that the tip could be placed selectively on either the periportal or the pericentral region of the liver lobule. This selective placement was possible because light areas and dark spots visible on the liver surface correspond, respectively, to periportal and pericentral regions (Fig. 1). Because the diameters of the periportal and pericentral regions (200–400 μm) are greater than that of the tip of the micro-light guide, it is possible to place the light guide on either region and measure pyridine nucleotide fluorescence changes.
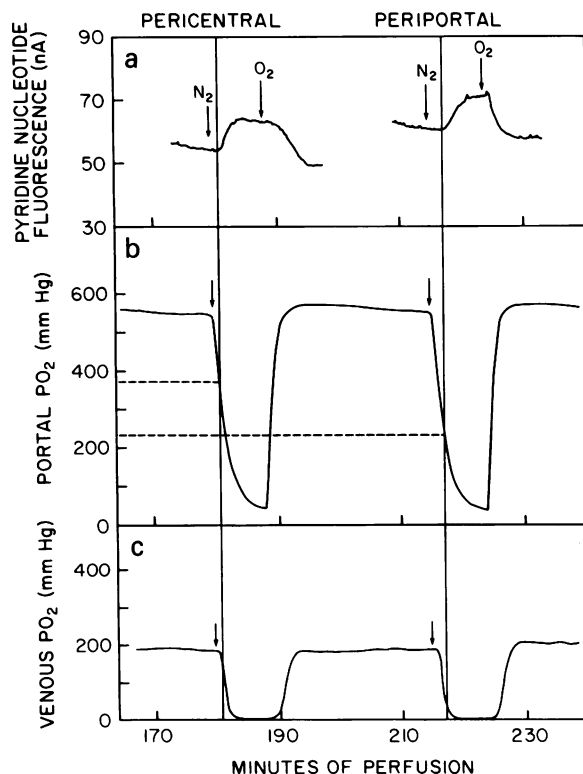
Table 2. Effects of chronic ethanol treatment on sublobular oxygen gradients and hepatic oxygen uptake: Reversal by 6-*n*-propyl-2-thiouracil (PrSur; PTU)

| Treatment | n | Oxygen gradient, torr | | | Rate of O₂ uptake, (μmol/g)/hr |
		Periportal	Pericentral	Lobular	
Sucrose	12	208 ± 13	67 ± 14	275 ± 20	110 ± 7
Ethanol	15	264 ± 19	136 ± 12*	400 ± 23*	144 ± 6†
Ethanol/PrSur	3	177 ± 27	53 ± 16	230 ± 19	118 ± 4

Procedures were similar to those in Fig. 2. Control rats were given 25% (wt/vol) sucrose in drinking water for 4–6 wk. Ethanol-treated rats were fed the Porta diet for 4–6 wk. Ethanol/PrSur-treated rats were given the Porta diet for 6 wk and then given PrSur plus the Porta diet for 3 to 4 more wk. PrSur was suspended in 1 ml of corn oil and administered by gastric incubation (50 mg/kg of body weight). Results are mean ± SEM.
* Significantly different from control; $P < 0.01$ (Student's t test).
† Significantly different from control; $P < 0.001$ (Student's t test).

If we assume that the pO_2 in the terminal portal venule (18) equals the pO_2 entering the cannulated portal vein, the influent pO_2 at which the pyridine nucleotide fluorescence begins to increase in pericentral areas can be regarded as the oxygen gradient across the liver lobule (lobular oxygen gradient). This follows from the fact that the pO_2 of the areas showing fluorescence increase will be virtually zero due to high affinity of cytochrome oxidase for oxygen (14, 26). Similarly, the influent pO_2 at which the pyridine nucleotide fluorescence begins to increase in periportal areas is equal to the oxygen gradient confined to the periportal portion of the liver lobule (periportal gradient).

Oxygen gradients calculated from direct pO_2 measurements made with the oxygen electrode were in excellent agreement with those calculated from optical data (Tables 2 and 3). Therefore, we conclude that the method for calculating oxygen gradients from inflow pO_2 values at which pyridine nucleotides become reduced is a valid means for investigating the lobular oxygen gradient in the perfused liver.

In addition to the lobular oxygen gradient, an intracellular oxygen gradient also exists (29–32). Chance and co-workers (29) estimated the intracellular oxygen gradient in isolated hemoglobin-free perfused rat heart by using a pair of oxygen-sensitive intracellular pigments, cytochrome a/a_3 and myoglobin. Based on the observation that both of these probes exhibited identical half-maximal responses when the oxygen tension was altered despite a 10-fold difference in their affinities for oxygen (0.1 vs. 1 torr), it was concluded that the intracellular oxygen gradient was very steep. Sies (31) carried out similar experiments using cytochrome a/a_3 and urate oxidase as intracellular probes for oxygen in the perfused liver and arrived at similar conclusions. Jones and Mason (32) used yet another method to estimate the intracellular oxygen gradient. They compared the apparent K_m

values of cytochrome a/a_3 for oxygen in isolated hepatocytes and mitochondria. Since the values were about one order of magnitude higher in hepatocytes than in mitochondria, they also concluded that a steep intracellular oxygen gradient exists.

If the intracellular oxygen gradient is sufficiently steep, it is possible that limited numbers of both periportal and pericentral cells coexist in the hypoxic state with the fraction of hypoxic cells per unit tissue volume increasing along the sinusoid in the direction of flow. However, anoxic zones could not be detected with the oxygen electrode in periportal regions of the perfused liver (unpublished results) nor did pyridine nucleotide fluorescence increase until the inflow oxygen tension was decreased from 600 to 200 torr in periportal areas (Table 2). Thus, in the perfused liver all regions of the liver lobule were most likely adequately supplied with oxygen. The possibility of periportal hypoxia is more likely *in vivo*, where inflow pO_2 values are less than 100 torr. More work is needed on this interesting possibility.

Effect of Ethanol Treatment on the Lobular Oxygen Gradient and Reversal by 6-Propyl-2-thiouracil. In sucrose-treated control livers, the lobular oxygen gradient was 275 torr measured optically and 357 torr measured with the oxygen electrode (Tables 2 and 3). The periportal gradient (208 and 278 torr) was considerably larger than the pericentral gradient (67 to 79 torr). This observation is consistent with the presence of larger mitochondria with more abundant cristae in periportal hepatocytes (33). In livers from chronically ethanol-treated rats, the lobular oxygen gradient increased to 400 torr measured optically and to 424 torr measured with the electrode. This increase in the oxygen gradient was accompanied by a similar increase in hepatic oxygen uptake and was confined primarily to the pericentral region of the lobule (Tables 2 and 3). This is of interest because ethanol causes pericentral injury in experimental ani-

Table 3. Direct measurement of sublobular oxygen gradients by using an oxygen minielectrode in perfused livers from sucrose- and ethanol-treated rats

| Treatment | Tissue pO_2, torr | | Oxygen gradient,* torr | | |
	Periportal	Pericentral	Periportal	Pericentral	Lobular
Sucrose	350 ± 49	271 ± 50	278 ± 50	79 ± 12	357 ± 50
Ethanol	347 ± 46	204 ± 47	281 ± 46	143 ± 14†	424 ± 47

Results are mean ± SEM.
* Calculated by assuming that the oxygen tension in the terminal portal venule is identical with the oxygen tension in the portal vein, which was 628 ± 11 torr. Mean venous oxygen tensions were 267 ± 23 and 228 ± 17 torr, respectively, for sucrose- and ethanol-treated groups. Rats were treated and livers were perfused as in Table 2. Tissue oxygen tensions were measured on the perfused liver surface by using an oxygen electrode. For each liver, 16 pairs of tissue pO_2 measurements were made in adjoint periportal and pericentral regions, and these values were averaged to obtain a single pair of mean periportal and pericentral tissue pO_2 values. These individual pairs of mean tissue pO_2 values from seven livers were then averaged to calculate the results.
† Significantly different from sucrose control; $P < 0.01$ (Student's t test).

mals and man. Presumably, the increase in hepatic oxygen uptake caused by ethanol treatment was also confined to the pericentral portion of the liver lobule. These results indicate that the increased oxygen uptake that results from chronic treatment with ethanol indeed increases the oxygen gradient along the sinusoid. These observations plus the fact that chronic ethanol treatment leads to a selective increase in the basal fluorescence intensity in pericentral regions (Table 1) indicate that pericentral hepatocytes are more vulnerable than periportal cells to ethanol-induced biochemical aberrations.

Israel and co-workers (4, 5) demonstrated that chronic treatment with ethanol increased the oxygen uptake of liver slices, a finding that was confirmed in the perfused rat liver (7, 8). However, one report that chronic treatment with ethanol does not enhance hepatic oxygen uptake has also appeared (34). Yuki and Thurman (8) have recently shown that enhanced hepatic oxygen uptake can occur very rapidly (in 2 to 3 hr) and is due, in part, to diminished ATP synthesis via glycolysis.

Israel *et al.* (3) also demonstrated that ethanol-treated rats are more susceptible to liver damage when exposed to hypoxia or ischemic shock than controls. They concluded that the elevated oxygen uptake of heptatocytes resulting from ethanol treatment accentuated the oxygen gradient and rendered the pericentral region of the liver lobule hypoxic. Further, they showed that the antithyroid drug 6-propyl-2-thiouracil reversed both the elevated hepatic oxygen uptake and most of the pericentral liver damage. 6-Propyl-2-thiouracil has subsequently been shown to reduce hepatic inflammation in chronic alcoholics (35). In recent experiments, we have demonstrated the possible role of the lobular oxygen gradient in the production of pericentral liver injury during hypoxia (36). In isolated perfused rat liver, low-flow hypoxia led to the formation of stable circumscribed zones of anoxia in pericentral regions. This anoxia rapidly caused severe hepatocellular injury confined to pericentral regions as determined by scanning and transmission electron microscopy. Thus, when oxygen delivery is insufficient to meet oxygen demand in the liver, anoxic zones developed around the central venules and led to pericentral cell injury.

6-Propyl-2-thiouracil prevents hypoxia-induced pericentral necrosis in livers from ethanol-treated rats (3) and also inhibits the "swift increase in alcohol metabolism" syndrome (37). We found that treatment of rats with 6-propyl-2-thiouracil abolished both the increase in tissue respiration and the enhanced pericentral oxygen gradient in perfused livers caused by chronic ethanol treatment (Table 2). These results provide evidence in support of the hypothesis that chronic ethanol treatment causes pericentral regions of the liver to become susceptible to hypoxia-induced cellular injury, as postulated by Israel *et al.* (3).

1. Schaffner, F. & Popper, H. (1970) *Scand. J. Gastroenterol.*, *Suppl. 7*, **5**, 69–78.
2. Galambos, J. T. (1972) in *Progress in Liver Diseases*, eds. Popper, H. & Schaffner, F. (Grune & Stratton, New York), pp. 567–588.
3. Israel, Y., Kalant, H., Orrego, H., Khanna, J. M., Videla, L. & Phillips, J. M. (1975) *Proc. Natl. Acad. Sci. USA* **72**, 1137–1141.
4. Videla, L., Bernstein, J. & Israel, Y. (1973) *Biochem. J.* **134**, 507–514.
5. Bernstein, J., Videla, L. & Israel, Y. (1973) *Biochem. J.* **134**, 515–521.
6. Israel, Y., Bernstein, H. & Videla, L. (1974) in *Alcohol and Aldehyde Metabolizing Systems*, eds. Thurman, R. G., Yonetani, T., Williamson, J. R. & Chance, B. (Academic, New York), pp. 493–509.
7. Thurman, R. G., McKenna, W. R. & McCaffrey, T. B. (1976) *Mol. Pharmacol.* **12**, 156–166.
8. Yuki, T. & Thurman, R. G. (1980) *Biochem. J.* **186**, 119–126.
9. Ji, S., Chance, B., Nishiki, K., Smith, T. & Rich, T. (1979) *Am. J. Physiol. Cell Physiol.* **52**, C144–C156.
10. Ji, S., Lüthen, G. & Kessler, M. (1979) in *Advanced Technobiology*, ed. Rybak, B. (Sijthoff-Noordhoff, Den Haag, The Netherlands), *NATO Adv. Study Inst. Ser. E Appl. Sci.* **31**, 237–268.
11. Ji, S., Lemasters, J. J. & Thurman, R. G. (1980) *FEBS Lett.* **113**, 37–41.
12. Ji, S., Lemasters, J. J. & Thurman, R. G. (1980) *FEBS Lett.* **114**, 349.
13. Chance, B., Mayevsky, A., Goodwin, C. & Mela, L. (1974) *Microvas. Res.* **8**, 276–282.
14. Chance, B. (1965) *J. Gen. Physiol.* **49**, 163–188.
15. Ji, S., Lemasters, J. J. & Thurman, R. G. (1980) *Pharmacol. Biochem. Behav. Suppl. 1*, **13**, 41–45.
16. Porta, E. A., Caesar, L. A. & Gomez-Dumm, S. A. (1968) *Lab. Invest.* **18**, 352–364.
17. Scholz, R., Hansen, W. & Thurman, R. G. (1973) *Eur. J. Biochem.* **38**, 64–72.
18. Rappaport, A. M. (1976) *Beitr. Pathol.* **157**, 215–243.
19. Krogh, A. (1918) *J. Physiol. (London)* **52**, 409–415.
20. Gonzalez-Fernandez, J. M. & Atta, S. E. (1968) *Math. Biosci.* **2**, 225–262.
21. Grünewald, W. A. & Sowa, W. (1977) *Rev. Physiol. Biochem. Pharmacol.* **77**, 149–209.
22. Grossman, U. & Lübbers, D. W. (1978) *Adv. Exp. Med. Biol.* **94**, 655–660.
23. Kessler, M., Höper, J. & Krumme, B. A. (1976) *Anaesthesiology* **45**, 184–197.
24. Kessler, M., Gornandt, L. & Lant, H. (1973) in *Oxygen Supply*, eds. Kessler, M., Bruley, D. F., Clark, L. C., Lübbers, D. W., Silver, I. A. & Strauss, J. (Univ. Park Press, Baltimore), pp. 156–159.
25. Chance, B., Cohen, P., Jöbsis, F. & Schoener, B. (1962) *Science* **137**, 1–10.
26. Oshino, N., Sugano, T., Oshino, R. & Chance, B. (1974) *Biochim. Biophys. Acta* **368**, 304–310.
27. Chance, B., Barlow, C., Haselgrove, J., Nakase, Y., Quistorff, B., Matschinsky, F. & Mayevsky, A. (1978) in *Microenvironments and Compartmentation*, eds. Srere, P. A. & Estabrook, R. W. (Academic, New York), pp. 131–148.
28. Matschinsky, F. M., Hintz, C. S., Reichlmeier, K., Quistorff, B. & Chance, B. (1978) in *Microenvironments and Compartmentation*, eds. Srere, P. A. & Estabrook, R. W. (Academic, New York), pp. 149–166.
29. Tamura, M., Oshino, N., Chance, B. & Silver, I. (1978) *Arch. Biochem. Biophys.* **191**, 8–22.
30. Oshino, N., Jamieson, D. & Chance, B. (1975) *Biochem. J.* **146**, 53–65.
31. Sies, H. (1978) *Adv. Exp. Med. Biol.* **94**, 561–566.
32. Jones, D. P. & Mason, H. S. (1978) *J. Biol. Chem.* **253**, 4874–4880.
33. Loud, A. V. (1968) *J. Cell Biol.* **37**, 27.
34. Schaffer, W. T., Penckla, W. D. & Veech, R. L. (1980) *Adv. Exp. Med. Biol.* **132**, 587–594.
35. Israel, Y., Walfish, P. G., Orrego, H., Blake, J. & Kalant, H. (1979) *Gastroenterology* **76**, 116–122.
36. Lemasters, J. J., Ji, S. & Thurman, R. G. (1981) *Science* **213**, 661–663.
37. Yuki, T., Israel, Y. & Thurman, R. G. (1982) *Biochem. Pharmacol.* in press.